AIP | Review of Scientific Instruments

Atomic resolution ultrafast scanning tunneling microscope with scan rate breaking the resonant frequency of a quartz tuning fork resonator

Quanfeng Li and Qingyou Lu

Citation: Rev. Sci. Instrum. **82**, 053705 (2011); doi: 10.1063/1.3585200
View online: http://dx.doi.org/10.1063/1.3585200
View Table of Contents: http://rsi.aip.org/resource/1/RSINAK/v82/i5
Published by the American Institute of Physics.

Related Articles

18/20 T high magnetic field scanning tunneling microscope with fully low voltage operability, high current resolution, and large scale searching ability
Rev. Sci. Instrum. 83, 043706 (2012)

Ultra compact multitip scanning tunneling microscope with a diameter of 50 mm
Rev. Sci. Instrum. 83, 033707 (2012)

Miniature active damping stage for scanning probe applications in ultra high vacuum
Rev. Sci. Instrum. 83, 033701 (2012)

A nanopositioner for scanning probe microscopy: The KoalaDrive
Rev. Sci. Instrum. 83, 023703 (2012)

Rapid measurement of a high step microstructure with 90° steep sidewall
Rev. Sci. Instrum. 83, 013706 (2012)

Additional information on Rev. Sci. Instrum.

Journal Homepage: http://rsi.aip.org
Journal Information: http://rsi.aip.org/about/about_the_journal
Top downloads: http://rsi.aip.org/features/most_downloaded
Information for Authors: http://rsi.aip.org/authors

ADVERTISEMENT

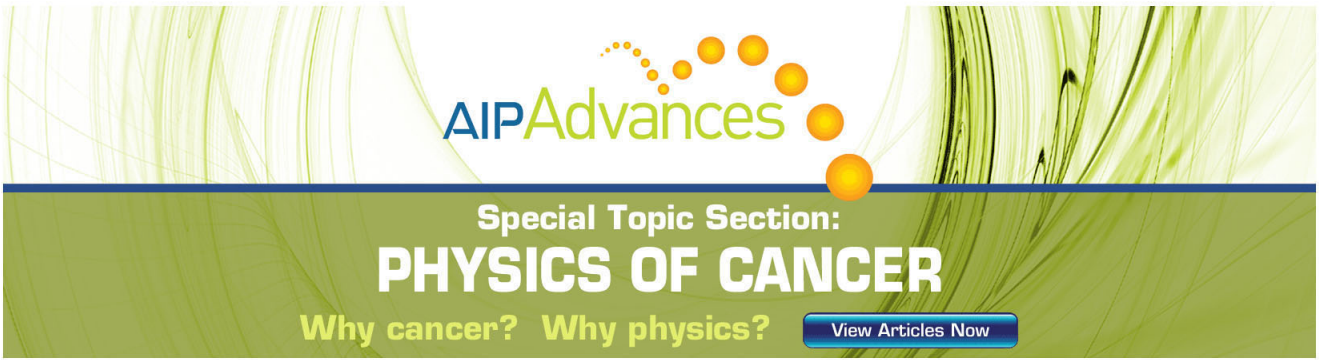

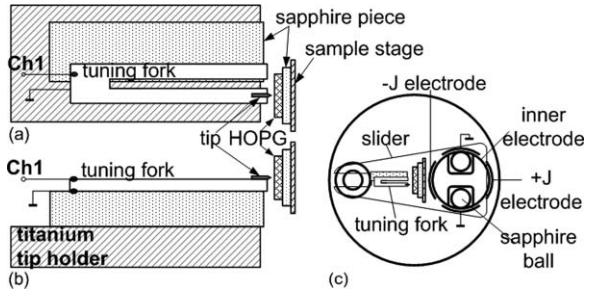

FIG. 1. The top view (a) and side view (b) of the tuning fork (fast scanner) and its position relative to the sample; (c) The top view of the STM's mechanical setup.

by the two prongs) lying horizontal. The STM tip is a hand-cut 0.15 mm thick Pt90/Ir10 wire (from Goodfellow), which is lengthwise glued (by H20E epoxy of Epoxy Technology) on the free prong of the fork with the tip protruding from the prong and pointing to the sample. The resonant frequency of the free tuning fork is 32.768 kHz which reduces to about 24 kHz when the tip is attached, and the quality factor is about 700 in ambient conditions, it can be oscillated well even in up to hundreds of kilohertz as fast axis (see Fig. 2).

Here, the tuning fork is in charge of the fast scan (along its vibration direction $\mathbf{H_F}$), whereas the slow scan (in direction $\perp_S$) is done by the scanner tube's axial displacement (faster than the traditional lateral-bending slow scan,[12,13] which is another advantage in achieving higher imaging speed).

The mass center of the slider is at the scanner side so that the slider motion well follows the scanner's control. The $\mathbf{H_J}$ direction oriented slot at the narrow end of the slider piece serves as the guide for the slider to slide toward the pillar ball by inertial steeping (coarse approach).[14] Because the tip-sample junction gap (in $\mathbf{H_J}$ direction) is now regulated by the scanner tube's lateral bending (large displacement per unit voltage) instead of the conventional axial deformation (small displacement per unit voltage), the coarse and fine approaches can be operated at low voltages (< 4 V), thus the whole STM is built with solely low voltage devices (power supply voltages $<$ the standard $\pm$15V),[11,12] which is very favorable to fast imaging.

III. CIRCUIT DESIGN

The traditional way to scan an image in constant height mode is as follows: a controller produces a pair of scan voltages ($V_X{}^C$, $V_Y{}^C$) to move the tip to a sample point neighboring to the previous point ⇆ measure the tunneling current I_T and record $V_X{}^C$, $V_Y{}^C$, I_T as the image data for that point. These two steps are repeated until enough sample area is measured and the set of ($V_X{}^C$, $V_Y{}^C$, $I_T{}^M$) data is used to form the image. Here, the superscripts C and M stand for controller output data (prearranged, not measured) and measured data, respectively, and the two-way arrow ⇆ indicates a repeated switch between these two data processing modes.

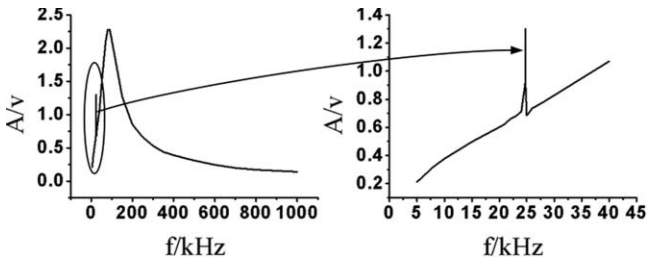

FIG. 2. The resonance curves of the tuning-fork fast scanner measured with the STM preamplifier (100 kHz bandwidth): (a) Covers the full measured frequency range from 0 to 1 MHz and (b) is a zoom-in of (a).

Our improvement is use a two-channel (Ch1 and Ch2) function generator to blindly vibrate the tuning fork (by signal V_X from Ch1, whose waveform is sinusoidal) for fast scan and blindly deform the scanner tube in its axial direction (by signal V_Y from Ch2, whose waveform is sinusoidal) for slow scan (the frequencies of the fast and slow scan satisfy $f_{fast} = N \times f_{slow}$, where N is the number of rows per frame) and blindly measure and record ($V_X{}^M$, $V_Y{}^M$, $I_T{}^M$) as image data (all are measured, no prearranged data).

The actual circuitry is Channel Ch1 of the function generator (Tektronix AFG3000) sends a sinusoidal wave V_X to a non-inverting reducer (by a factor of 0.18) circuit whose output drives the tuning fork to perform fast scan (in $\mathbf{H_F}$ direction) through the mechanical vibration of the free prong (Fig. 1). Channel Ch2 outputs another slower sinusoidal wave V_Y, which is first attenuated by an inverting reducer (by a factor of 0.1) circuit and then applied to the inner electrode of the scanner tube (see Fig. 3) for slow scan.

A real time computer (National Instruments PXI-8106 RT with PXI-7851R data acquisition card) blindly measures and records ($V_X{}^M$, $V_Y{}^M$, $I_T{}^M$) data from both channels Ch1, Ch2, and the STM preamplifier (see Fig. 3), respectively. The STM preamplifier has a bandwidth of about 100 kHz with a $R_F = 10$ MOhm feedback resistor in the transimpedance amplifier. Since the computer only acquires data and does not

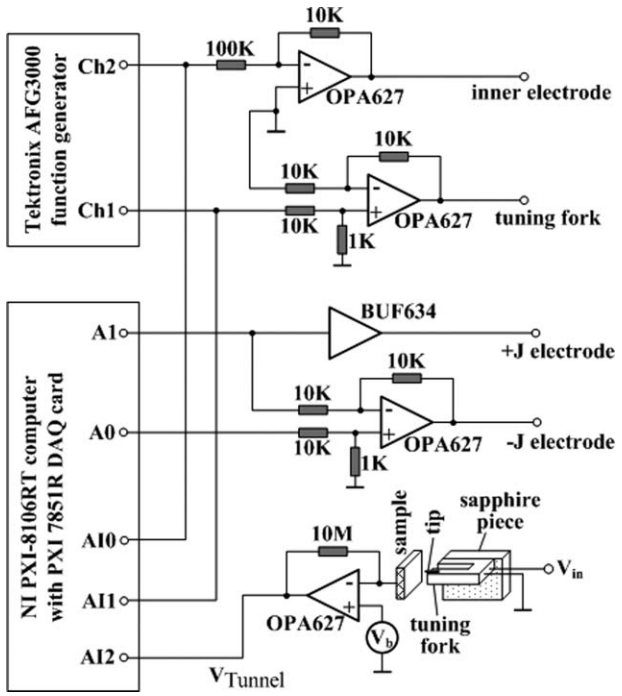

FIG. 3. The schematic drawing of the electronic system that drives the electrodes of the scanner tube and tuning fork and collects the imaging data.

Downloaded 15 Jul 2012 to 211.86.158.23. Redistribution subject to AIP license or copyright; see http://rsi.aip.org/about/rights_and_permissions

output any scan signal to move the tip, there is no switch between acquiring and outputting and therefore the imaging speed can be greatly increased. We can see from the above circuit system that no high voltage devices or instruments are used. All voltages are less than ±15V.

Our real time computer is actually rather slow: its maximum data acquisition speed is only 520 thousand data per channel per second (520 kHz/Ch). We have indeed tried the traditional point-by-point scan-and-measure imaging mode (with a switch between each data acquisition and data output) using this computer and found the maximum data acquisition speed drops to 40 kHz/Ch. We will also show that in this mode the atoms in the image become completely invisible at 3 kHz scan rate due to the lack of enough pixels (only 3 pixels per pixel line are acquired). However, with our new blind-scan-blind-measure method, the atoms are still clearly visible even at a scan rate as high as 26 KHz, which is beyond the resonant frequency (24 kHz) of the fork resonator (see Sec. IV).

IV. EXPERIMENTAL RESULTS

The performance of our tuning fork resonator ultra-fast STM has been tested by imaging a highly oriented pyrolytic graphite (HOPG) (GYBS/1.7, type ZYB from NT-MDT) sample in air at room temperature. For comparison, we first scanned the sample in traditional mode: using the computer as the controller to repeatedly (1) output a pair of scan voltages (V_X and V_Y) to move the tip to a new position and then (2) measured and recorded I_T data. Figure 4 shows the so obtained images at a series of scan rates of 57, 909, 2000, and 3300 Hz. Each atomic row only contains three atoms because the driving voltage applied on the tuning fork is low and the scan rate is far below the resonant frequency of the fork, which cannot invoke a large prong vibration amplitude.

It is easily seen from Fig. 4 that as the scan rate goes higher and higher, the number of pixels per pixel-line reduces, making the atoms look more and more mosaicked. This failure mode implies that the data acquisition rate is too low under this traditional mode. Our solution is to get rid of all the switches between I_T acquisition and scan motion and make the computer do nothing but acquire data. The scan motion can be solely implemented by a function generator. Under this "blind scan and blind acquire" mode, we first obtained a HOPG atomic image at 13 kHz scan rate (Fig. 5, constant height mode with 50 mV sample positive bias voltage) which is not only the highest scan rate in literature that still holds atomic resolution but also shows better image quality.

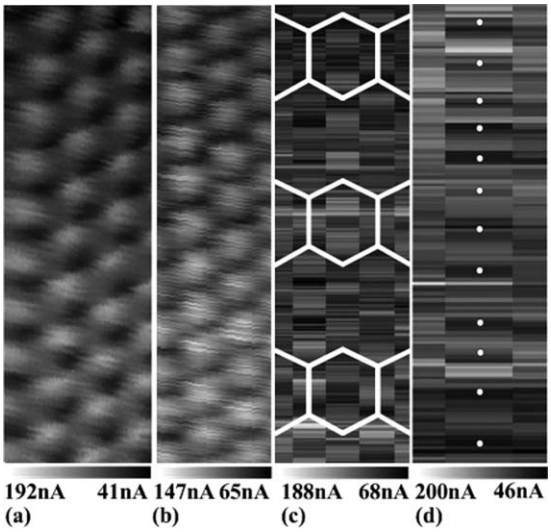

FIG. 4. A series of HOPG STM images (raw data) taken in air with increasing scan rate using the traditional point-by-point scan and data acquisition mode. Image conditions are (a) 57 Hz, 0.68 × 2.34 nm^2, 177 × 477 pixels; (b) 909 Hz, 0.50 × 2.58 nm^2, 11 × 600 pixels; (c) 2 kHz, 0.59 × 2.71 nm^2, 5 × 800 pixels, lattice barely seen and (d) 3.3 kHz, 0.52 × 3.08 nm^2, 3 × 10 000 pixels, atomic lines barely seen.

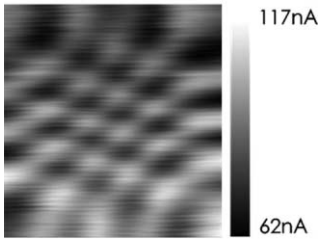

FIG. 5. The atomically resolved HOPG STM image (raw data) taken in air using the proposed uninterrupted scan and uninterrupted data acquisition mode (under conditions: 13 kHz scan rate, 1.07 × 0.98 nm^2 scan size, 52 Hz frame rate, tuning fork driven by $V_{P\text{-}P}$ = 1.82 V sine wave, 20 × 250 pixels, 520 kHz sampling rate).

Now, we are in a position to increase the scan rate further. Figure 6 is the atomic resolution HOPG image at 26 kHz, which already exceeds the resonant frequency of the tuning fork resonator. The scan size in the fast scan direction is low because we knew the scan rate was close to the speed limit of the data acquisition and reduced the scan size on purpose by using a low fork driving voltage of 1.2 V. Also, the nanometer target searching capability across the entire sample for this microscope[10] should solve any scan size issue if needed.

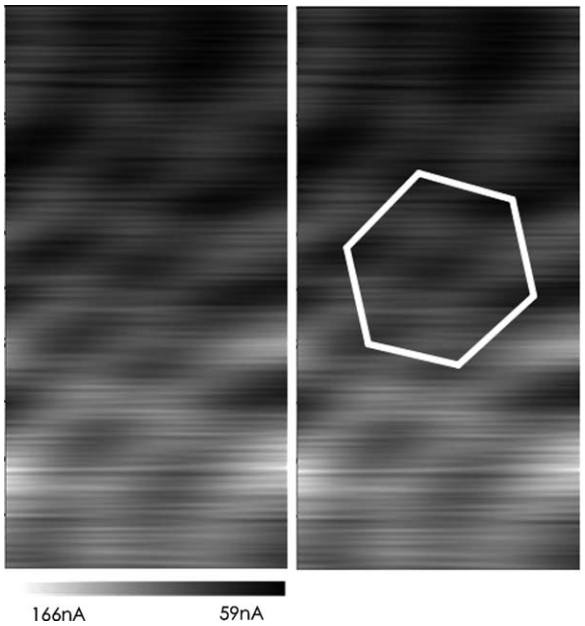

FIG. 6. Atomically resolved HOPG STM image (raw data) in air at 26 kHz scan rate. The right hand size image is the same as the left one except that one unit cell is marked. Image size is 0.53 × 1.23 nm^2, tuning fork driving voltage is $V_{P\text{-}P}$ = 0.22 V sine wave, pixel number is 10 × 250, sampling rate is 520 kHz.

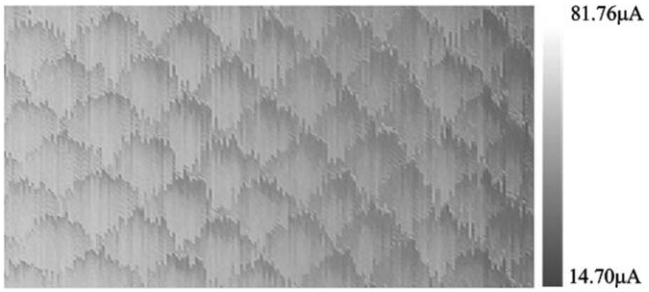

FIG. 7. Atomically resolved HOPG STM image taken with an ultralow feedback resistor (= 10 k Ohm) showing the possibility of achieving atomic resolution images with faster preamplifier, image size is 1.72 × 1.23 nm^2.

Since the graphite atoms can still be resolved at 26 kHz scan rate and the only issue is lower pixel number per pixel-line, we surely expect that this problem can be easily solved by using a faster data acquisition card. It is worthwhile mentioning that the STM preamplifier is not a limiting factor because we have obtained atomic resolution HOPG images (see Fig. 7, in which the atoms are flakelike and the lattice is skewed into square type from hexagonal, which is due to distortion and can be corrected by spiral scan[18]) using a feedback resistor as low as $R_F = 10$ k Ohm, which has a potential bandwidth much higher than the 100 kHz used here. Also, there are other technologies in literature that can enhance the bandwidth of the preamplifier. One example is to use the STM junction itself (which has high resistance and low parasitic capacitance, thus providing a great bandwidth) to convert the weak tunneling current into a strong voltage signal. We proposed this idea and filed a patent application in 2006[19] and in 2007 similar idea led to a radio-frequency STM[6] (which unfortunately did not show any atomic resolution image).

It will be very interesting to see what failure mode at what scan rate will show up first if we use a data acquisition card much faster than 520 kHz.

V. CONCLUSION

We have presented a tuning fork resonator ultra-fast STM that can provide atomic resolution at 26 kHz. The proposed fully low voltage design and "blind scan and blind data acquisition" make it possible for the scan rate to go beyond the resonant frequency of the resonator. The only failure mode seen is lower pixel number per pixel-line. Using a faster data acquisition card will presumably achieve unforeseeable high imaging speed without losing atomic resolution.

ACKNOWLEDGMENTS

This work was supported by the National Natural Science Foundation of China under Grant No.10627403, the Science Foundation of The Chinese Academy of Sciences under Grant No. YZ200846 and the project of Chinese national high magnetic field facilities.

[1] G. Binnig, H. Rohrer, Ch. Gerber, and E. Weibel, Phys. Rev. Lett. **50**, 120 (1983).
[2] D. M. Rampulla, A. J. Gellman, and David S. Sholl, Surf. Sci. **600**, 2171 (2006).
[3] M. J. Rost, L. Crama, P. Schakel, E. van Tol, G. B. E. M. van Velzen-Williams, C. F. Overgauw, H. ter Horst, H. Dekker, B. Okhuijsen, M. Seynen, A. Vijftigschild, P. Han, A. J. Katan, K. Schoots, R. Schumm, W. van Loo, T. H. Oosterkamp, and J. W. M. Frenken, Rev. Sci. Instrum. **76**, 053710 (2005).
[4] H. J. Mamin, H. Birk, P. Wimmer, and D. Rugar, J. Appl. Phys. **75**, 161 (1994).
[5] S. O. Reza Moheimani, Rev. Sci. Instrum. **79**, 071101 (2008).
[6] U. Kemiktarak, T. Ndukum, K. C. Schwab, and K. L. Ekinci, Nature **450**, 85 (2007).
[7] T. Ando, *Roadmap of Scanning Probe Microscopy* (Springer, Berlin, Heidelberg, 2007).
[8] J. C. Vickerman and I. S. Gilmore, *Surface Analysis - The Principal Techniques*, 2nd ed. (Wiley, New York, 2009).
[9] H. Neddermeyer, Rep. Prog. Phys. **59**, 701 (1996).
[10] Z. Q. Pang, J. H. Wang, and Q. Y. Lu, Meas. Sci. Technol. **20**, 065503 (2009).
[11] Y. B. Hou, J. H. Wang, and Q. Y. Lu, Rev. Sci. Instrum. **79**, 113707 (2008).
[12] C. R. Ast, M. Assig, A. Ast, and K. Kern, Rev. Sci. Instrum. **79**, 093704 (2008).
[13] S. A. Zareian Jahromi, M. Salomons, Q. Sun, and R. A. Wolkow, Rev. Sci. Instrum. **79**, 076104 (2008).
[14] M. Jayadevaiah and V. Lakshminarayanan, Meas. Sci. Technol. **15**, 35 (2004).
[15] D. Croft, G. Shed, and S. Devasia, J. Dyn. Syst., Meas., Control **123**, 35 (2001).
[16] G. Schitter and A. Stemmer, IEEE Trans. Control. Syst. Technol. **12**(3), 449 (2004).
[17] F. J. Giessibl, Rev. Mod. Phys. **75**, 949 (2003).
[18] J. T. Wang, J. H. Wang, Y. B. Hou, and Q. Y. Lu, Rev. Sci. Instrum. **81**, 073705 (2010).
[19] Q. Y. Lu, P. R. China patent No. 200610097197.0 (2006).